Magnetic and Transport Properties of $Ba_6Fe_8S_{15}$ and $BaFe_2S_3$: Magnetoresistance in a Spin-Glass-Like Fe(II) System

Z. Serpil Gönen,[†] Patrick Fournier,[‡] Vera Smolyaninova,[‡] Richard Greene,[‡] Fernando M. Araujo-Moreira,[§] and Bryan Eichhorn*[,†]

Departments of Chemistry and Physics, Center for Superconductivity Research, University of Maryland, College Park, Maryland 20742, and Departamento de Física-Grupo de Supercondutividade e Magnetismo, UFSCar—Universidade Federal de São Carlos, São Carlos/SP, 13565-905 Brazil

Received January 14, 2000. Revised Manuscript Received July 13, 2000

The magnetic and transport properties of the Hong and Steinfink 1-dimensional barium iron sulfide phases $BaFe_2S_3$ and $Ba_6Fe_8S_{15}$ were studied. The valence precise $BaFe_2S_3$ phase (Fe^{2+}) is semiconducting with a nonmagnetic ground state due to strong intrachain antiferromagnetic coupling. However, short-range magnetic correlations and spin-glass-like behavior are found below 25 K, which gives rise to a magnetoresistive effect of 10% at 9 T. $BaFe_2S_3$ is a rare example of a magnetoresistive ternary sulfide. The mixed valent $Ba_6Fe_8S_{15}$ phase ($Fe^{2.25+}$) is also a semiconductor with a nonmagnetic ground state. $Ba_6Fe_8S_{15}$ shows similar spin-glass-like behavior but at a lower temperature ($T_f = 15$ K). Comparisons with other tetrahedrally coordinated iron sulfide phases and possible origins of the short-range magnetic correlations are discussed.

Introduction

Background. Recent investigations have shown that large magnetoresistive (MR) effects can be found in a variety of non-oxide compounds. Ramirez and co-workers[1,2] have shown that a large MR effect is present in the chromium spinels, ACr_2S_4, where A = Fe, Cu, Cd. These compounds represent a distinct class of MR phases that are semiconducting ferromagnets at all temperatures and do not appear to be mixed valent.[1,2] In most MR materials, ferromagnetism (or canted antiferromagnetism) is observed and the maximum MR effect is usually found near T_c.[3,4] In contrast, Kauzlarich and co-workers have discovered magnetoresistive behavior in transition metal Zintl compounds, such as $Eu_{14}MnBi_{11}$, where antiferromagnetic ordering is clearly present in some cases.[5−7]

The observation of magnetoresistance in the Cr spinels and Zintl compounds has shown that perovskites are not the only compounds demonstrating MR effects. These studies have also proven that mixed valency and the double-exchange mechanism are not unifying explanations for the observed magnetic and resistivity properties of magnetoresistive compounds. Furthermore, the observed MR effects in the semiconducting spin glasses[8,9] and the antiferromagnetic Zintl compounds[5] show that metallic behavior and traditional three-dimensional ferromagnetism are also not stringent requirements for a sizable MR response.

To further investigate the occurrence of magnetoresistivity in mixed valent and valence precise compounds outside the realm of perovskite oxides, we have been studying the ternary sulfides of the first row transition metals. Herein, we report the magnetic and transport properties of the Hong and Steinfink compounds[10] $Ba_6Fe_8S_{15}$ and $BaFe_2S_3$. Although the room-temperature susceptibility and resistivity studies of these compounds have been reported,[11] their low-temperature properties have not been investigated. We report here that both compounds are semiconductors that show short-range magnetic correlations and are spin-glass-like at low temperatures. In addition, $BaFe_2S_3$ shows a small magnetoresistive effect (10%) below 25 K.

Experimental Section

All sample manipulations were conducted in a nitrogen atmosphere, in a drybox. $BaCl_2$ and CsCl were recrystallized from aqueous HCl, dried under vacuum, and stored in the

* To whom correspondence should be addressed.
[†] Department of Chemistry, University of Maryland.
[‡] Department of Physics, University of Maryland.
[§] Universidade Federal de São Carlos.

(1) Ramirez, A. P.; Cava, R. J.; Krajewski, J. *Nature* **1997**, *386*, 156.
(2) Ramirez, A. P. *J. Phys.: Condens. Matter.* **1997**, *9*, 8171.
(3) Raveau, B.; Maignan, A.; Caignaert, V. *J. Solid State Chem.* **1995**, *117*, 424.
(4) Maignan, A.; Caignaert, V.; Simon, C.; Hervieu, M.; Raveau, B. *J. Mater. Chem.* **1995**, *5*, 1089.
(5) Chan, J. Y.; Kauzlarich, S. M.; Klavins, P.; Shelton, R. N.; Webb, D. J. *Phys. Rev. B* **1998**, *57*, R8103.
(6) Chan, J. Y.; Wang, M. E.; Rehr, A.; Kauzlarich, S. M.; Webb, D. J. *Chem. Mater.* **1997**, *9*, 2131.
(7) Chan, J. Y.; Kauzlarich, S. M.; Klavins, P.; Shelton, R. N.; Webb, D. J. *Chem. Mater.* **1997**, *9*, 3132.
(8) Pérez, J.; García, J.; Blasco, J.; Stankiewiez, J. *Phys. Rev. Lett.* **1998**, *80*, 2401.
(9) Groult, D.; Martin, C.; Maignan, A.; Pelloquin, D.; Raveau, B. *Solid State Commun.* **1998**, *105*, 583.
(10) Hong, H. Y.; Steinfink, H. *J. Solid State Chem.* **1972**, *5*, 93.
(11) Reiff, W. M.; Grey, I. E.; Fan, A.; Eliezer, Z.; Steinfink, H. *J. Solid State Chem.* **1975**, *13*, 32.

10.1021/cm0000346 CCC: $19.00
Published on Web 10/12/2000

drybox. All other reagents were purchased from CERAC and used without further purification. For the reactions requiring the use of flux, silica ampules were carbon coated by reducing acetone inside the tube at high temperature.

Synthesis. Both of the title compounds were prepared using slight modifications of the procedures of Hong and Steinfink.[10]

$BaFe_2S_3$. 0.245 g of BaS, 0.162 g of Fe, and 0.093 g of S (1:2:2 mole ratio) were ground in the presence of 20% (w/w) $BaCl_2$:CsCl eutectic flux, loaded into a carbon-coated silica ampule, and sealed under vacuum. The mixture was heated according to the following schedule:

$$\text{RT} \xrightarrow{1°/\text{min}} 300\ °\text{C} \xrightarrow{5\ \text{h}} 300\ °\text{C} \xrightarrow{1°/\text{min}} 790\ °\text{C} \xrightarrow{48\ \text{h}} 790\ °\text{C} \xrightarrow{\text{quench}} \text{RT}$$

The sample was quenched to room temperature in water. The product was washed with ethanol several times to remove the flux. The isolated powder was black and crystalline. Without flux in the reaction mixture, $Ba_6Fe_8S_{15}$ and other unidentified products were obtained. Slow cooling resulted in the formation of the desired product but small amounts of unidentified impurities were always present.

$Ba_6Fe_8S_{15}$. 0.290 g of BaS, 0.128 g of Fe, and 0.082 g of S (6:8:9 mole ratio) were intimately ground and loaded into a carbon-coated silica ampule in a drybox. The ampule was then sealed under vacuum and put into a furnace. The sample was heated to 760 °C (1 °C/min) and held at this temperature for 48 h. The ampule was quenched to room temperature in water, yielding a highly crystalline black powder.

Characterization. X-ray powder diffraction (XRD) patterns were recorded using a Rigaku DMAX B powder X-ray diffractometer and an MDI software system. Rietveld analyses of the XRD patterns were used to assess sample identities and purities. The single-crystal X-ray data of Hong and Steinfink were used as starting models.[10] General refinement procedures used in our laboratories have been described elsewhere.[12]

Variable temperature and variable field dc magnetic susceptibilities were measured using a Quantum Design MPMS superconducting quantum interference device (SQUID) magnetometer. For these measurements, polycrystalline samples were loaded into gelatin capsules. For zero-field-cooled (ZFC) experiments, the samples were loaded into the magnetometer at room temperature and subsequently cooled to 5 K before energizing the magnetic field. Magnetization decay curves were measured by warming the sample above $T = 50$ K, cooling the sample to the final temperature (30 or 5 K) in the zero field, applying the field ($H = 1.0$ T) for $t = 300$ s, turning the field off, and then measuring the magnetization as a function of time. ac susceptibility measurements were performed by using a high-sensitivity custom-made susceptometer in the conventional configuration with frequencies between 1.0 and 1000.0 Hz, an excitation magnetic field up to 4.0 Oe, external magnetic fields up to 5 T, and a temperature range of $2 < T < 400$ K.

Resistance measurements were carried out in the temperature range of 4.2−300 K for $BaFe_2S_3$ and $Ba_6Fe_8S_{15}$ by using a standard four-probe technique. The compounds were pressed into cylinders using the multianvil high-pressure furnace (50 kbar, 400 °C for 5 h). The cylinders were cut into rectangular blocks and gold wires were attached to the samples with silver paste. To decrease the contact resistance, samples were annealed under vacuum at 400 °C prior to resistance measurements.

EDX studies were performed on polycrystalline samples using a JEOL 840 scanning electron microscope equipped with a microprobe attachment.

Results

Single-phase $BaFe_2S_3$ was prepared by quenching the sample to room temperature after heating at 790 °C to avoid the formation of $Ba_6Fe_8S_{15}$ formed during slow cooling. Single-phase $Ba_6Fe_8S_{15}$ can be prepared by slow cooling the sample; however, superior crystallinity is obtained by quenching. EDX analysis of the samples indicated only Ba, Fe, and sulfur, indicating that chloride from the flux was not incorporated into the lattice.

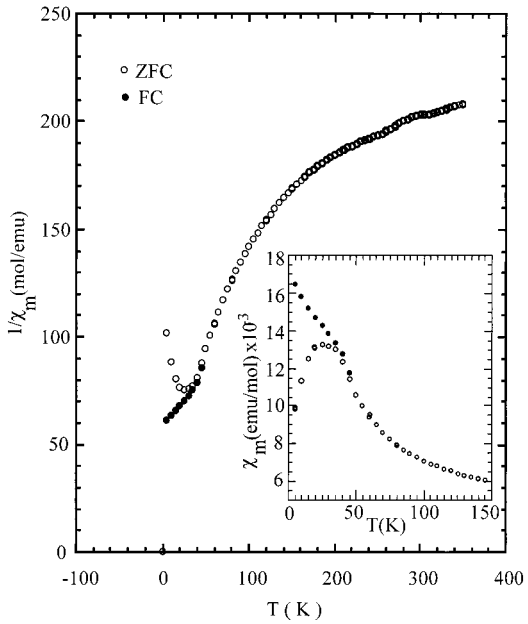

Figure 1. Plot of inverse molar magnetic susceptibility vs temperature for $BaFe_2S_3$ showing zero-field-cooling (ZFC) and field-cooling (FC) data at 100 Oe (inset, ZFC and FC magnetic susceptibilities between 5 and 150 K).

The calculated and observed XRD patterns for $BaFe_2S_3$ and $Ba_6Fe_8S_{15}$ are given in the Supporting Information. Although observed and calculated XRD patterns agree very well for $Ba_6Fe_8S_{15}$, slight intensity differences were observed for some reflections in the observed pattern of $BaFe_2S_3$. These differences are presumably due to a slight preferred orientation. However, SEM analysis indicated single-phase material and single-crystal X-ray diffraction on a selected crystal confirmed the composition and structure. The low-temperature crystal structure (100 K) is identical to the room-temperature structure,[10] indicating the absence of a structural phase transition.

Magnetic and Transport Properties. *$BaFe_2S_3$*. The magnetic susceptibility of $BaFe_2S_3$, measured at 100 Oe, is shown in Figure 1. Below 25 K, the divergence of the field-cooled susceptibility, FC, and zero-field-cooled susceptibility, ZFC, illustrates the absence of long-range magnetic order. However, the cusp at 25 K (freezing temperature, T_f) indicates the presence of short-range magnetic correlations and spin-glass-like behavior below 25 K. The plot of magnetization versus field at 5 K (below T_f) shows hysteresis with a coercive field of 1.8 kOe and a small remnant moment of 0.0623 emu/g (Figure 2). The FC and ZFC data do not coincide at temperatures slightly above T_f (25 K $< T <$ 50 K), which could indicate the presence of magnetic clusters in this range. Above 50 K, the FC and ZFC values of the susceptibility are the same and magnetization curves ($M(H)$) do not exhibit hysteresis or a remnant moment. Therefore, the compound is assumed to be paramagnetic above 50 K. However, the plots of reciprocal susceptibil-

(12) Tranchitella, L.; Chen, B. H.; Fettinger, J. C.; Eichhorn, B. W. *J. Solid State Chem.* **1997**, *130*, 20.

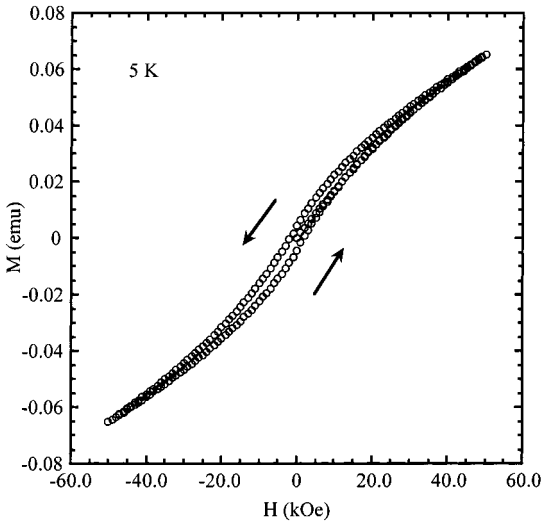

Figure 2. Plot of magnetization versus field for $BaFe_2S_3$ at 5 K.

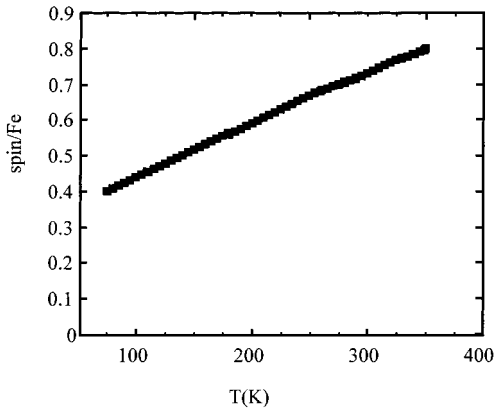

Figure 3. Plot of spin per iron versus temperature for $BaFe_2S_3$.

ity versus temperature are nonlinear above 50 K, indicating that the compound is not a simple Curie–Weiss paramagnet. Fits of the data to the Curie–Weiss law that include a term for temperature-independent paramagnetism, χ_i (eq 1), gave unreasonably large values for that term (e.g., $\approx 10^{-2}$ emu/mol). We attribute

$$\chi_m = \chi_i + \frac{C}{T - \theta} \tag{1}$$

the origin of the nonlinearity to temperature-dependent variable spin of the Fe ions, as has been seen in related manganese and iron sulfides studied by Bronger et al.[13–15] Assuming the Weiss constant, θ, is zero, we can estimate the average spin per Fe ion in the paramagnetic region from the following expression:

$$\chi_m = \frac{Ng^2\beta^2 S_{(T)}(S_{(T)} + 1)}{3kT} \tag{2}$$

This analysis gives an average spin state of $S = 0.8$ per iron at 350 K and $S = 0.4$ at 80 K (Figure 3). The susceptibility data give a room-temperature effective

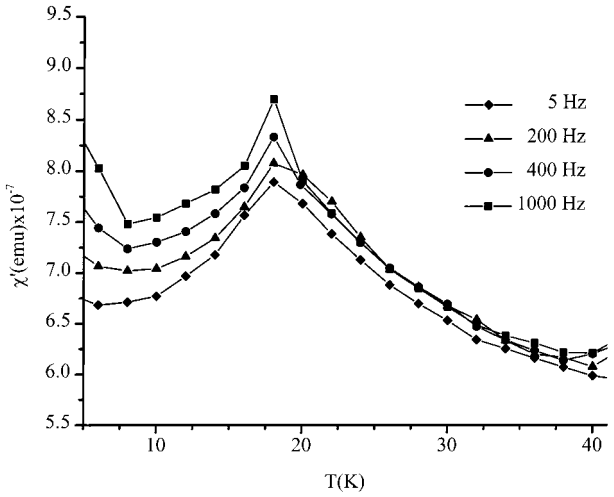

Figure 4. Plot of ac magnetic susceptibility vs temperature for $BaFe_2S_3$ recorded at different frequencies.

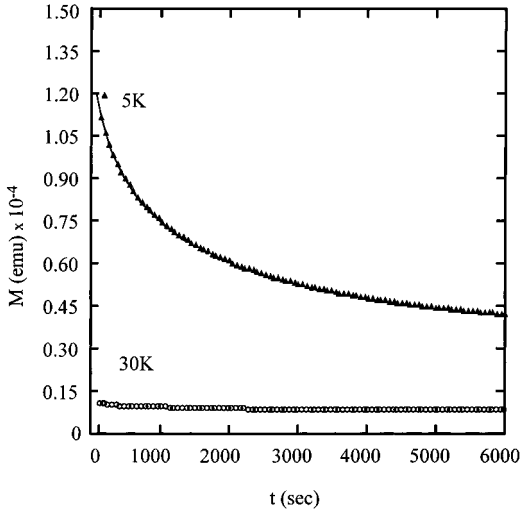

Figure 5. Plot of remnant magnetization versus time for $BaFe_2S_3$ at 5 and 30 K. The solid lines connecting the data points are fits to eq 3.

magnetic moment (μ_{eff}) of 2.23 μ_B per Fe. A Gouy balance measurement gave a similar value (μ_{eff} = 2.01 μ_B per Fe).

To confirm the presence of spin-glass-like short-range magnetic correlations in $BaFe_2S_3$, low-temperature ac susceptibility studies were conducted at 3.8 Oe (Figure 4). The data show a frequency dependence due to the short-range magnetic correlations, which is consistent with the dc susceptibility studies. However, there is no discernible change in the location of the cusp as the frequency is changed. Magnetization decay curves at 30 and 5 K (Figure 5) also show spin-glass-like behavior characteristic of short-range magnetic correlations. The 5 and 30 K data were fit to the stretched exponential equation,[16]

$$M = M_2 + (M_1 - M_2)\exp\left(-\left(\frac{t}{\tau}\right)^{\beta}\right) \tag{3}$$

where M_1 is the initial magnetization, M_2 is the final magnetization, t is the delay time in seconds, τ is the

(13) Bronger, W. *Ber. Bunsen-Ges. Phys. Chem.* **1992**, *96*, 1572.
(14) Bronger, W. *Angew. Chem., Int. Ed. Engl.* **1981**, *20*, 52.
(15) Bronger, W.; Kyas, A.; Müller, P. *J. Solid State Chem.* **1987**, *70*, 262.
(16) Palmer, R. G.; Stein, D. L.; Abrahams, E.; Anderson, P. W. *Phys. Rev. Lett.* **1984**, *53*, 958.

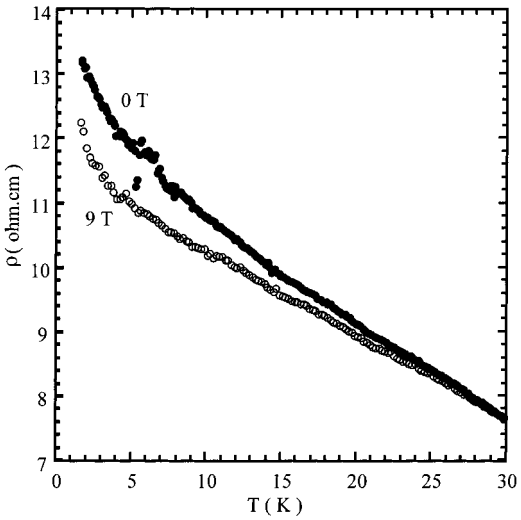

Figure 6. Low-temperature resistivity of $BaFe_2S_3$ at different applied magnetic fields.

relaxation constant in seconds, and β can take on values from 0 (constant M, no relaxation) to 1 (usual exponential relaxation).[17] The fit of the 5 K data give $\tau = 1.2 \times 10^3$ s and $\beta = 0.54$. This stretched exponential behavior indicates the presence of various relaxation times corresponding to different barriers, which is typical for spin-glass-like systems.

The plot of resistivity versus temperature for $BaFe_2S_3$ shows semiconductor-like behavior with room-temperature resistivity of ≈0.35 Ω·cm. A fit of the log R versus $1/T$ data to the expression

$$R = R_0 e^{E_g/2kT} \quad (4)$$

gives a band gap of 0.06(1) eV. This value is in excellent agreement with the 0.07-eV gap reported by Reiff et al. from single-crystal measurements.[11]

The resistivity of $BaFe_2S_3$ below 25 K is magnetic-field-dependent as shown in Figure 6. The resistivity shows a negative magnetoresistance of ≈10% in a field of 9 T at ≈5 K. Because the magnetoresistance is not very large in this material, it is possible that its origin is the loss of spin-disorder scattering, which was observed previously in magnetic semiconductors.

$Ba_6Fe_8S_{15}$. The magnetic susceptibility of $Ba_6Fe_8S_{15}$ is shown in Figure 7 and is essentially temperature-independent between 100 and 350 K. The low-temperature data also show a divergence in FC and ZFC susceptibility consistent with spin-glass-like short-range magnetic order. However, the lower T_f value (15 K) and the large resistivity of the compound (≈10^7 Ω·cm at 40 K) precluded analysis of the MR response. The plot of magnetization versus field at 50 K shows paramagnetic behavior that was similar to that of $BaFe_2S_3$ described above. Fitting the susceptibility data to eq 1 also gave unreasonably large temperature-independent contributions, which is consistent with a variable spin system. If we assume that the material is paramagnetic throughout the 50−350 K temperature range, we can estimate the average spin value per Fe ion from eq 2. This analysis gives an average spin state of $S = 1.2$ per iron at 350 K and $S = 0.5$ at 100 K as shown in Figure 8.

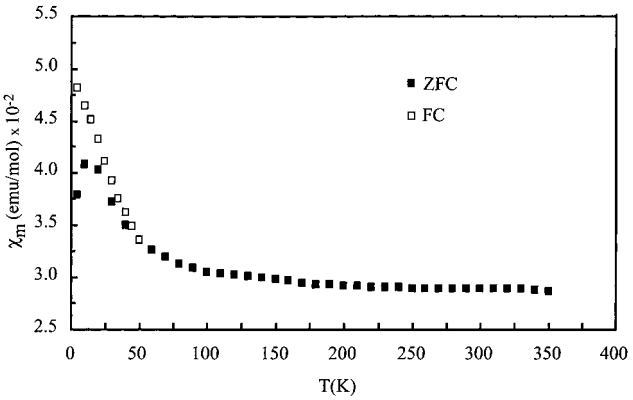

Figure 7. Plot of molar magnetic susceptibility vs temperature for $Ba_6Fe_8S_{15}$ showing zero-field-cooling (ZFC) and field-cooling (FC) data at 100 Oe.

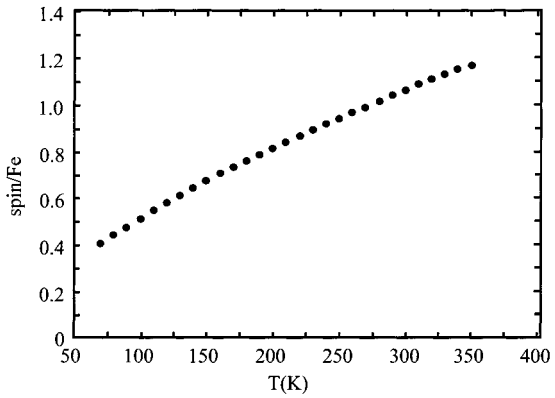

Figure 8. Plot of spin (S) per iron versus temperature for $Ba_6Fe_8S_{15}$.

The temperature dependence of the resistivity for $Ba_6Fe_8S_{15}$ shows typical semiconductor behavior with a room-temperature resistivity of ≈0.73 Ω·cm. The high-temperature data are linear in the plot of log R versus $1/T$ and give a band gap of 0.33(1) eV. Again, this value is in excellent agreement with the 0.31-eV gap previously reported for this compound by Reiff et al.[11] It is interesting to note that the low-temperature resistivity of $Ba_6Fe_8S_{15}$ is several orders of magnitude larger than that of $BaFe_2S_3$.

Discussion

Before proceeding with a discussion of the physical properties, it is necessary to review the structural aspects of the two compounds. $Ba_6Fe_8S_{15}$ is tetragonal, space group $I4/m$, and contains tetrahedrally coordinated iron in Fe_4S_{10} clusters (Figure 9a) that form chains running parallel to the c-axis (Figure 9b).[10] The clusters can be viewed as an octahedral array of eight sulfur atoms (bolded lines in Figure 9a) with four of the eight faces capped by Fe−S groups. The S_8 octahedral arrays share corners along the c-axis. The chains are separated by nine-coordinate Ba^{2+} ions. The Fe atoms are formally mixed valent with six Fe^{2+} and two Fe^{3+} per formula unit. However, there is only one crystallographic Fe site, suggesting that the charge is delocalized to give an average iron oxidation state of +2.25. In contrast, $BaFe_2S_3$ contains only Fe^{2+} ions in tetrahedral

(17) Mydosh, J. A. *Spin Glasses: An Experimental Introduction*; Taylor & Francis: London, 1993.

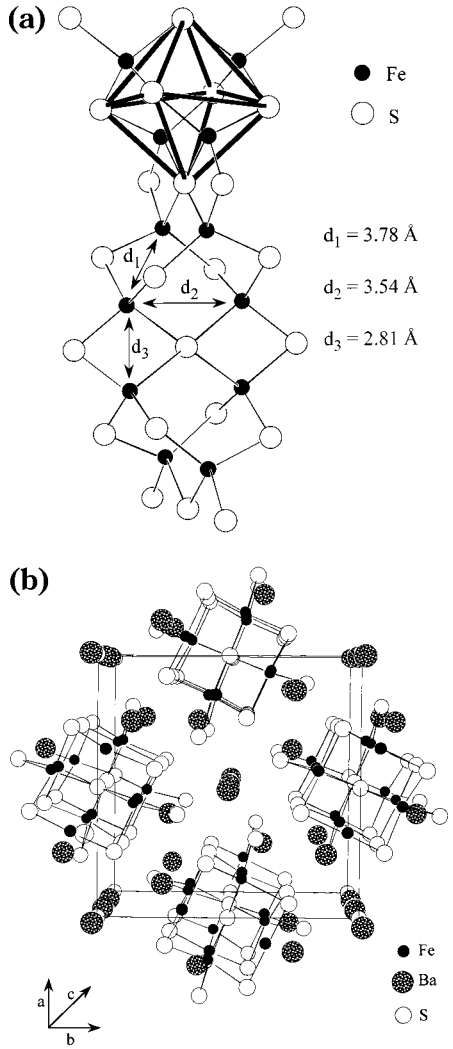

Figure 9. Crystal structure of $Ba_6Fe_8S_{15}$ showing (a) the Fe_4S_{10} clusters forming a chain parallel to the *c*-axis and (b) a view of the clusters down the *c*-axis.

coordination environments. Its structure is orthorhombic, space group *Cmcm*, and contains double chains of edge-sharing tetrahedra running parallel to the *c*-axis (Figure 10a).[10] Each FeS_4 tetrahedron shares three edges with neighboring tetrahedra. The chains are separated by eight-coordinate Ba^{2+} ions (Figure 10b).

Both $BaFe_2S_3$ and $Ba_6Fe_8S_{15}$ have tetrahedral iron centers coordinated by the relatively weak-field sulfur atoms. On the basis of a simple crystal field argument, one might expect high spin states for both compounds with $S = 2$ for the Fe(II) compound $BaFe_2S_3$ and a higher average spin state for the mixed valent $Ba_6Fe_8S_{15}$, which formally contains both Fe(II) and Fe(III). The observed susceptibilities for both compounds give values of approximately $S = 1$ per iron at room temperature and approximately $S = 0.5$ at 100 K (see Figures 3 and 8). The observed nonmagnetic ground states can be understood by considering two factors. First, the short intrachain Fe−Fe contacts in both compounds (2.81 Å for $Ba_6Fe_8S_{15}$ and 2.64−2.70 Å for $BaFe_2S_3$) have been shown by Bronger et al. to significantly perturb the crystal field splitting in related compounds.[13] The limit of these direct Fe−Fe interactions result in the formation of metal−metal bonds.[18] These concepts were first put forward by Goodenough

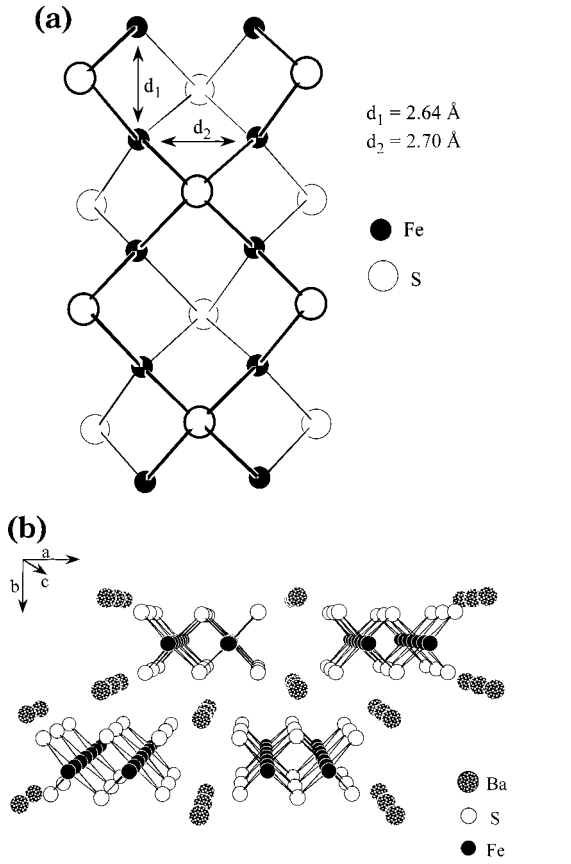

Figure 10. Crystal structure of $BaFe_2S_3$ showing (a) the chains of double tetrahedra running parallel to the *c*-axis and (b) a view of the chains down the *c*-axis.

et al. in their correlation of structural and electronic properties with extensive Mössbauer studies.[19−21] For reference, Fe−Fe bonds are as short as 2.177(3) Å[22] in low valent organometallics; however, at slightly longer distances, such as the 2.265(1) Å Fe−Fe distance in $(\eta^5\text{-}C_5Me_5)_2Fe_2(CO)_2H$, electron pairing in metal−metal bonds is incomplete and paramagnetic ground states are observed.[23] The second factor to consider is the strong antiferromagnetic coupling of the ions that is mediated through the sulfide ions. The combination of antiferromagnetic coupling, additional crystal field splitting due to neighboring Fe atoms, and direct Fe−Fe interactions presumably give rise to $S = 0$ ground states in these compounds. Similar nonmagnetic ground states have been observed in A_3FeS_3 and $AFeS_2$ phases (A = alkali) containing isolated Fe_2S_6 double tetrahedra and edge-shared tetrahedral chains, respectively.[14,15] In this regard, the magnetic data are consistent with expectations based on comparisons with the alkali iron sulfides. However, our calculated moments (for $BaFe_2S_3$, μ_{eff} = 2.23 μ_B; for $Ba_6Fe_8S_{15}$, μ_{eff} = 2.95 μ_B) are significantly

(18) Cotton, F. A.; Walton, R. A. *Multiple Bonds Between Metal Atoms*, 2nd ed.; Oxford University Press: New York, 1993.
(19) Goodenough, J. B. *Mater. Res. Bull.* **1978**, *13*, 1305.
(20) Goodenough, J. B. *J. Solid State Chem.* **1982**, *41*, 1.
(21) Fatseas, G. A.; Goodenough, J. B. *J. Solid State Chem.* **1980**, *33*, 219.
(22) Murahashi, S.-I.; Mizoguchi, T.; Hosokawa, T.; Moritani, I.; Kai, Y.; Kohara, M.; Yasuoka, N.; Masai, N. *J. Chem. Soc., Chem. Commun.* **1974**, 563.
(23) Blaha, J. P.; Bursten, B. E.; Dewan, J. C.; Frankel, R. B.; Randolph, C. L.; Wilson, B. A.; Wrighton, M. S. *J. Am. Chem. Soc.* **1985**, *107*, 4561.

lower than the essentially spin-only moments originally reported by Reiff et al.

Both the valence precise $BaFe_2S_3$ and the mixed valent $Ba_6Fe_8S_{15}$ compounds show short-range magnetic correlations and spin-glass-like behavior at low temperatures despite the dominate antiferromagnetic interactions in these compounds. The occurrence of a transition in which spin orientations freeze without establishing long-range order requires that the magnetic sublattice exhibit a high degree of randomness or geometry favoring frustration and the spins be subject to strongly competing interactions. These conditions are satisfied in some amorphous compounds as well as in materials with crystalline structures characterized by some combination of magnetic site disorder and a geometry favoring frustration.[24−26] Without additional magnetic data, one can only speculate as to the origin of the short-range magnetic correlations in $BaFe_2S_3$ and $Ba_6Fe_8S_{15}$. The spin freezing temperature is similar to the antiferromagnetic ordering temperature of Na_5FeS_4 ($T_N = 28$ K), which has Fe−Fe separations of 5.98 Å.[27] For comparison, each iron atom in $BaFe_2S_3$ has two 5.86 Å and two 6.09 Å interchain contacts. $Ba_6Fe_8S_{15}$ has shorter interchain contacts of 5.36 and 5.65 Å. In addition, the long-range connectivities between the Fe centers in the two compounds are quite similar. On the basis of these observations, we propose that each $^1_\infty[Fe_2S_2]^{2-}$ chain possess *intra*chain antiferromagnetic coupling with a nonmagnetic ground state. However, *inter*chain interactions appear at low temperature that give rise to short-range magnetic correlations and a small magnetoresistive effect.

The magnetoresistance in $BaFe_2S_3$ is of course very small in comparison with the manganites and the Kauzlarich phases.[5−7] However, it is a rare example of a magnetoresistive ternary sulfide that, in contrast to most MR materials, is a one-dimensional semiconductor with spin-glass-like short-range correlations.[5]

Acknowledgment. This work was funded by the NSF through Grants DMR 9223060 and DMR 9732736. We thank Mr. Scott Sirchio for the WDS data.

Supporting Information Available: Calculated and observed XRD patterns of $Ba_6Fe_8S_{15}$ and $BaFe_2S_3$. This material is available free of charge via the Internet at http://pubs.acs.org.

CM0000346

(24) Bodénan, F.; Cajipe, V. B.; Danot, M.; Ouvrard, G. *J. Solid State Chem*. **1998**, *137*, 249.
(25) Binder, K.; Young, A. P. *Rev. Mod. Phys.* **1986**, *58*, 4.
(26) Cai, J. W.; Wang, C.; Shen, B. G.; Zhao, J. G.; Zhan, W. S. *Appl. Phys. Lett.* **1997**, *71*, 1727.
(27) Klepp, K. O.; Bronger, W. *Z. Anorg. Allg. Chem*. **1986**, *532*, 23.